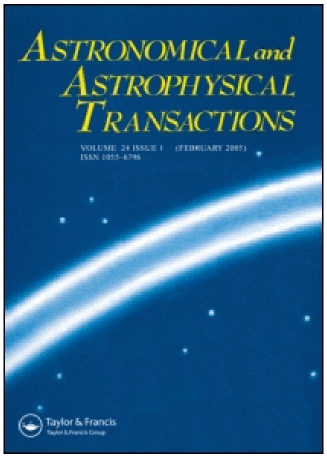

Astronomical & Astrophysical Transactions
The Journal of the Eurasian Astronomical Society
Publication details, including instructions for authors and subscription information:
http://www.informaworld.com/smpp/title~content=t713453505

Solar flare dynamics obtained by X-ray observations

Porfir'eva; Yakunina

Online Publication Date: 01 January 2003
To cite this Article: Porfir'eva and Yakunina (2003) 'Solar flare dynamics obtained by X-ray observations', Astronomical & Astrophysical Transactions, 22:4, 611 - 616
To link to this article: DOI: 10.1080/1055679031000098529
URL: http://dx.doi.org/10.1080/1055679031000098529

Astronomical and Astrophysical Transactions
Vol. 22, Nos. 4–5, August–October 2003, pp. 611–616

SOLAR FLARE DYNAMICS OBTAINED BY X-RAY OBSERVATIONS

G. PORFIR'EVA* and G. YAKUNINA

Sternberg Astronomical Institute, Lomonosov Moscow State University, Universitetskij Prospekt 13, Moscow 119992, Russia

(Received November 12, 2002)

The dynamic properties of solar flares are considered on the basis of the spectral observations of soft X-rays of more than 180 flares obtained during the last two decades. The random non-thermal velocities are in the range from 60 to 580 $\mathrm{km\,s^{-1}}$ but mainly change from 110 to 190 $\mathrm{km\,s^{-1}}$. The mean value of the ξ calculated for flares being mainly of C1-M5 X-ray classes are equal to $160.8 \pm 4.7\,\mathrm{km\,s^{-1}}$. The directed velocities in flares are from several dozen to several hundred kilometres per second. The relationships between ξ and other flare characteristics are discussed. Investigations of flare dynamics help us to understand the nature of energy transport in them.

Keywords: Sun; Corona; Flares; Plasma motions

1 INTRODUCTION

Flares are highly dynamic processes on the Sun. The hot plasma of the flare moves along the magnetic flux tubes with velocities of several dozen to several hundred of kilometres per second. High-resolution X-ray spectra from the Japanese Yohkoh spacecraft were obtained with a higher sensitivity and time resolution in comparison with previous cosmic flare investigations. Simultaneous spectral and spatial observations from Yohkoh permitted us to analyse the morphology and dynamics of solar flares in more detail. Preflare phase spectra were recorded with a 24 s integration time and flare spectra had a 3–9 s time resolution. The SXT telescope operated with 2.45″ spatial resolution. In this paper, data on the velocities of directed and chaotic motions in the corona during flares are considered and the relations between the velocities, electron temperature T_e and X-ray emission are analysed. Literature data have been used.

2 OBSERVATIONS

The velocities and temperature of the flare plasma are derived from spectral line parameters. On the Yohkoh, narrow wavelength ranges around the X-ray lines of the S XV (5.04 Å), Ca XIX (3.18 Å) and Fe XXV (1.85 Å) ions were recorded. The Yohkoh BCS (Bragg Crystal

*Corresponding author.

ISSN 1055-6796 print; ISSN 1476-3540 online
DOI: 10.1080/1055679031000098529

Spectrometer) spectrometer was uncollimated and therefore the entire flare was observed without spatial resolution. The line profiles were the profiles integrated through the region occupied by the flare. For time moments near the flare onset the line profiles are noticeably wider and displaced compared with the decay phase profiles. The Doppler shifts from the standard line wavelength give the line-of-sight velocities V_{ls} of the flare plasma. The additional linewidth, in comparison with the thermal linewidth, is considered as a result of non-thermal chaotic motions. A flare line profile can be represented by a Gaussian (or Voigt) profile or a sum of Gaussian profiles. After correcting for instrumental broadening the Doppler half-width $\Delta\lambda_D$ of an optically thin line is related to the temperature T by the equation

$$\frac{\Delta\lambda_D}{\lambda}c = \left(\frac{2kT_i}{M_i} + \xi^2\right)^{1/2},$$

where c is the speed of the light, λ is the standard wavelength of the emission line, M_i is the mass of the ion producing the line and k is the Boltzmann constant. The non-thermal velocity ξ is the excess amount of the observed linewidth over the thermal contribution $V_{th} = (2kT_i/M_i)^{1/2}$ and it is often considered as a turbulent velocity. The electron temperature T_e of the flare was derived from the ratios of the satellite to resonance lines intensities of the corresponding ions (Feldman et al., 1980) and represented an average over all the flare region.

During the flare onset the line profiles have complex shapes. In Figure 1, soft X-ray (SXR) images of the flares with different morphologies are shown. The upward chromospheric evaporation is believed to fill with plasma magnetic tubes and to be responsible for line shifts. As was discussed by Nitta et al. (1999) and Porfir'eva et al. (2001), knowledge of the spatial

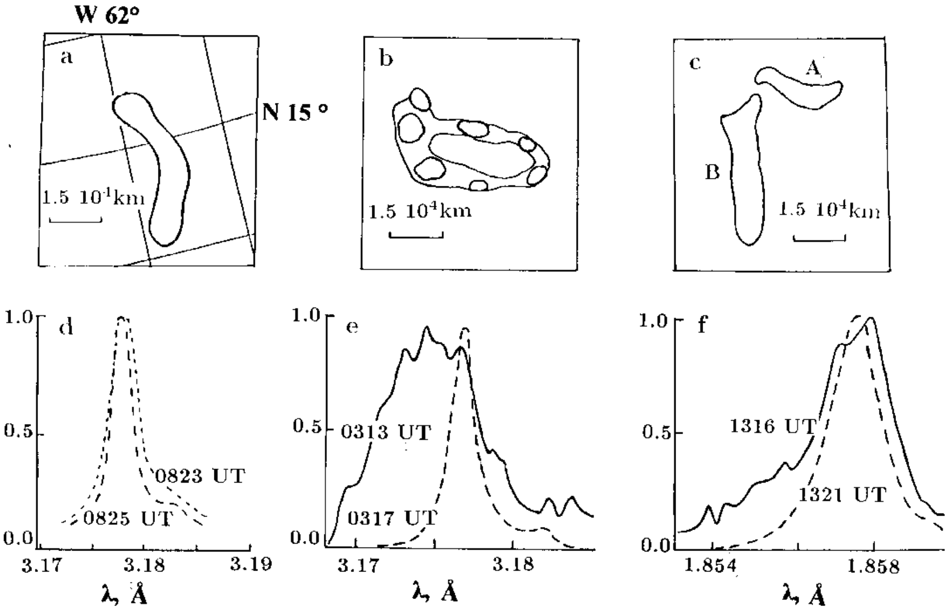

FIGURE 1 Schematic drawing of the flares with different morphologies (a) on August 22, 1992, obtained by Porfir'eva et al. (2001), (b) on November 9, 1991, obtained by Doschek et al. (1994) and (c) on January 5, 1992, obtained by Doschek et al. (1993), together with the corresponding profiles of (d), (e) Ca XIX and (f) Fe XXV lines. The red- (dotted) and blue-shifted (solid) lines together with non-shifted (dashed) lines and their times of the observation are shown. In their peaks the line profiles are normalized to 1.

flare loop geometry is important for line profile interpretation. If the morphology of the flare is simple and we see a single flare loop situated in a plane, then we can evaluate the plasma velocity in space, knowing the loop geometry and V_{ls}. The blue or red shift of the line depends on the inclination of the loop plane to or from the observer. As was discussed by Sterling et al. (1996) an upward evaporation flow can appear to be apparently moving away as projected on the line of sight. If the morphology of the flare is complex, it is very difficult to analyse the line profiles properly.

In Figure 1 we see an example of a simple flare structure and simple line profile and two other examples of complex flares. For convenience of the comparison the line profiles in their peak intensity are normalized to 1. The flare of August 22, 1992, had a loop shape (Fig. 1(a)). The flare of November 9, 1991, looked like a ring with bright emission spots situated along the ring (Fig. 1(b)), which changed their locations and brightness very quickly (Doschek et al., 1994). The character of the change differed for the different flare spots. The line profile had a winding shape and was highly blue shifted (Fig. 1(e)) at the onset of the flare. The flare of January 5, 1992, had two main loops A and B and several details of minor importance (Fig. 1(c)). Loop A flared first and had a sigmoid shape (S-shaped loop) and loop B flared later. The line profiles were blue shifted (Fig. 1(f)) during the onset of the flare, then the blue shift decreased but, some minutes later, when loop B brightened, the blue shift increased again.

The complex line profiles are decomposed into moving and stationary components (see for example Doschek et al. (1993; 1994)). Different physical features may be assumed when flare line profiles are decomposed. The main assumption is that the temperatures of the moving and stationary plasma are the same. More often the moving component is considered to consist of a single component (Doschek et al., 1993; 1996), but sometimes it is decomposed into more than one component (Doschek et al., 1994). The spectral width of the moving component is assumed to be the same as the stationary component width or different from it (Doschek et al., 1994), or to be proportional to the Doppler shift from the standard wavelength (Fludra et al., 1989; Nitta et al., 1999). If the spectral widths of the moving and stationary components are supposed to be not equal, the widths are determined by decomposing the observed line profiles, and as a rule the moving components appear to be wider than the stationary components. The moving flare plasma is likely to have more random motions than the stationary plasma does.

3 RESULTS AND THEIR DISCUSSION

For the flare of November 9, 1991, during the first 18 s, T_e was in the range from 14×10^6 to 17×10^6 K, the upward flow velocity V_{ls} changed from 200 to 400 km s^{-1}, the non-thermal velocities were in the range from 310 to 580 km s^{-1} and in the range from 70 to 130 km s^{-1} for the moving (ξ_m) and stationary (ξ_s) components respectively, depending on the wavelength. At the onset of the flare the ratios of the emission measure of the moving component to that of the stationary component were from 4 to 25 for the different ions. In this flare the moving component was dominated by the stationary component in many times. At the onset of the M1.9 flare, which occurred on January 5, 1992, $12 \times 10^6\ \mathrm{K} < T_e < 18 \times 10^6\ \mathrm{K}$, $210\ \mathrm{km\,s^{-1}} < V_{ls} < 250\ \mathrm{km\,s^{-1}}$, $330\ \mathrm{km\,s^{-1}} < \xi_m < 480\ \mathrm{km\,s^{-1}}$, $110\ \mathrm{km\,s^{-1}} < \xi_s < 140\ \mathrm{km\,s^{-1}}$ and the ratios of the intensity of the moving component to that of the stationary component changed from 0.75 to 0.9; that is, in this case the stationary component was very strong relative to the moving component. Other parameters of the flares of January 5, 1992, and November 9, 1991, were comparable.

The ξ value changes noticeably during the flare. It was revealed that ξ begins to increase before the onset of the flare, reaches its peak and then decreases to the usual level in the active region (AR) (of about 20–40 km s^{-1}) when there is no flare in it (Sterling, 1997;

Harra et al., 2001). Different lines show different electron temperatures T_e, flow velocities V_{ls} and non-thermal velocities ξ. Because we have integrated line profiles, it is difficult to understand such a result. However, it is possible that the flare plasma is not homogeneous in its temperature and motions and consists of tiny volumes or threads differing in their characteristics. Also, different volumes of the flare can give different contributions to the line profile. To understand the flares better, we need spectra with a better space resolution.

We compiled results of different investigations and believe that the flare non-thermal velocity is described by its peak ξ_{max}. In Figure 2 the histograms for the non-thermal velocities ξ_{max} are shown. All flares were divided into two groups, with $T_e > 10^7$ K and $T_e < 10^7$ K. For the first group the ξ_{max} values are in the range from 110 to 190 km s^{-1}, and the average $\bar{\xi}_{max} = 161.1 \pm 3.0$ km s^{-1}. For weaker flares included in the second group, ξ_{max} ranged from 100 to 150 km s^{-1}, and the mean $\bar{\xi}_{max} = 146.4 \pm 8.4$ km s^{-1}. The hotter flares (the first group) have higher non-thermal velocities. About 200 values were used in the first case and 40 values in the second case. The mean random velocity $\bar{\xi}_{max}$ for all flares without dividing them into two temperature groups is equal to 160.8 ± 4.7 km s^{-1}.

Each flare is characterized by a set of ξ according to measurements on different X-ray lines. We obtained the results for a definite flare in only one investigation. If any flare was analysed in different papers, we had to choose only one result or took the mean value of the two results. The non-thermal velocities for both the moving and the stationary components were included. In all papers used, the flares of weak and mean X-ray classes were used, because for very strong flares some difficulties are possible in the interpretation of the line profiles owing to intensity saturation effects.

The non-thermal velocity correlates best of all with the hard-X-ray (HXR) emission. The peak ξ values coincide in time approximately with the peak in HXRs. As shown by Ranns et al. (2001), systematic differences are observed in the non-thermal velocity ξ behaviour in flares with different characters of time increase in the HXR brightness. The non-thermal velocity has a tendency to peak before the HXR emission peak, if the flare brightness increases gradually and, after that, if there is an impulsive increase in the HXR emission. An analysis of 59 flares of classes C2.8 and M6.1, 35 of which were flares that increased gradually and 24 were flares that increased in an impulsive manner, revealed that the time

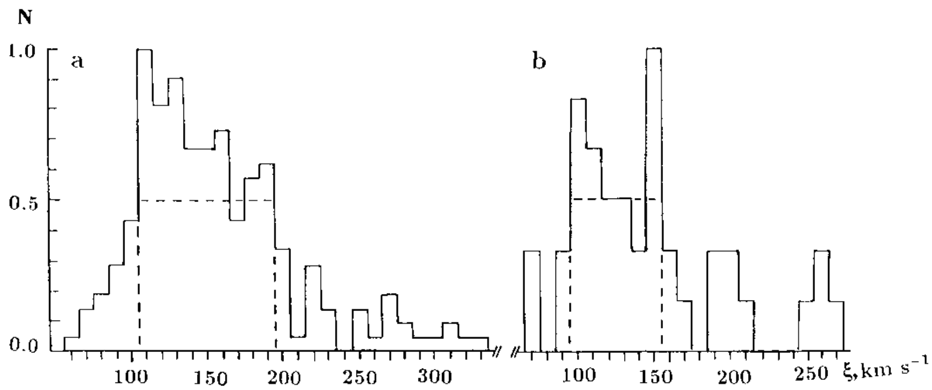

FIGURE 2 Histograms of maximum non-thermal velocities ξ for (a) hot flares with $T_e > 10^7$ K and (b) weak flares with $T_e < 10^7$ K, with their peaks normalized to 1. The data on the observations used in (a) are from Antonucci et al. (1984), Fludra et al. (1989), Doschek et al. (1994; 1996), Antonucci and Podero (1995), Khan et al. (1995), Mariska et al. (1996), Harra-Murnion et al. (1997), Sterling (1997), Alexander et al. (1998), Mariska and McTiernan (1999), Nitta et al. (1999), Ranns et al. (2000; 2001) and Harra et al. (2001); those in (b) are from Antonucci and Dodero (1995) and Harra-Murnion et al. (1997).

delay between the peaks of the non-thermal velocity ξ and HXR emission is about 10–30 s for the impulsively increasing flares and about 50–100 s for the gradually increasing flares (Ranns et al., 2001). It is likely that there is a clear tendency for the impulsively increasing flares to manifest a shorter delay time than the gradually increasing flares. There are examples when, the longer the HXR burst lasts after its maximum, the longer the enhanced level of the non-thermal velocity is preserved. In some flares, ξ has secondary peaks associated with secondary HXR peaks. Also the ξ time behaviour can show some fluctuations with an amplitude of the order of 10–20 km s^{-1}, that is greater than the average error in ξ of several kilometres per second, as discussed by Harra et al. (2001) for the events on October 3, 1993.

The ξ–HXR relation is likely to occur not by chance and indicates a close connection of the physical processes, causing the increase in the non-thermal velocity, with the processes triggering the flare. In the paper by Harra et al. (2001), observations of two solar flares occurred in AR 7590 on October 3, 1993, within an 18 min interval are presented. The increase in ξ above the usual background level in the AR began 11 min before the start of the second flare. For these 11 min, ξ increased gradually by a factor of 2. As indicated by Harra et al. (2001), the initial increase in ξ before the flare onset shows that there is preflare turbulence, associated with the process that eventually leads to the flare. It is possible that reconnection of magnetic field lines is such a process.

Fludra et al. (1989) studied the relationship between the directed velocity V_{ls} and the chaotic velocity ξ. In some flares with intense upward plasma flows a correlation of the random and directed motions has been found. The larger ξ correspond to the larger V_{ls}, although generally they are weakly correlated.

The line-of-sight velocities V_{ls} observed during the flares are in the range from several dozen to several hundred kilometres per second but we must remember that V_{ls} is only a part of the full directed velocity because of projection effects. The non-thermal velocities ξ are also in the range from several dozen to several hundred kilometres per second. For the moving component the ξ values are often greater than V_{ls}. The random velocity in the moving component (ξ_m) is always greater than in the stationary component (ξ_s). Probably the moving and stationary plasma components occupy different regions in the flare body.

Analysis of the flares with different heliographic coordinates show no dependence of the non-thermal velocity ξ on the flare location on the solar disc. The non-thermal plasma motions are likely to be isotropic in space (Mariska, 1994). The SXR emission, temperature and emission measure increase more slowly than HXR emission does and reach their peak later than the non-thermal velocity does.

Until now the physical nature of non-thermal line broadening has not been clear. The most perspective mechanism explaining the additional broadening of flare lines is magnetohydrodynamic turbulence although other explanations are possible. So Antonucci et al. (1996) discussed an approximation of reconnecting current sheets in the flare region. The outflows that originate during the reconnection process can result in non-thermal broadening in the flare SXR lines.

The creation of models allowing for real processes in solar flares is a difficult task. Modern spectral X-ray observations do not give answers to many questions. Observation of X-ray spectra with a better space resolution would help us to understand better the flare nature on the Sun.

References

Alexander, D., Harra-Murnion, L., Khan, J. and Matthews, S. (1998). Astrophys. J., 494, L235.
Antonucci, E., Benna, C. and Somov, B. V. (1996). Astrophys. J., 456, 833.
Antonucci, E. and Dodero, M. A. (1995). Astrophys. J., 438, 480.

Antonucci, E., Gabriel, A. H. and Dennis, B. R. (1984). Astrophys. J., 287, 917.
Doschek, G. A., Mariska, J. T. and Sakao, T. (1996). Astrophys. J., 459, 823.
Doschek, G. A., Mariska, J. T., Strong, K. T., Bentley, R. D., Brown, C. M., Culhane, J. L., Lang, J., Sterling, A. C. and Watanabe, T. (1994). Astrophys. J., 431, 888.
Doschek, G. A., Strong, K. T., Bentley, R. D., Brown, C. M., Culhane, J. L., Fludra, A., Hiei, E., Lang, J., Mariska, J. T. and Philips, K. J. H. (1993). Astrophys. J., 416, 845.
Feldman, U., Doschek, G. A. and Kreplin, R. W. (1980). Astrophys. J., 238, 365.
Fludra, A., Lemen, J. R., Jakimiec, J., Bentley, R. D. and Sylwester, J. (1989). Astrophys. J., 344, 991.
Harra, L. K., Matthews, S. A. and Culhane, I. L. (2001). Astrophys. J., 549, L245.
Harra-Murnion, L. K., Akita, K. and Watanabe, T. (1997). Astrophys. J., 479, 464.
Khan, J. I., Harra-Murnion, L. K., Hudson, H. S., Lemen, J. R. and Sterling, A. C. (1995). Astrophys. J., 452, L153.
Mariska, J. T. (1994). Astrophys. J., 434, 756.
Mariska, J. T. and McTiernan, J. M. (1999). Astrophys. J., 514, 484.
Mariska, J. T., Sakao, T. and Bentley, R. D. (1996). Astrophys. J., 459, 815.
Nitta, N., van Driel-Gesztelyi, L. and Harra-Murnion, L. K. (1999). Solar Phys., 189, 181.
Porfir'eva, G. A., Yakunina, G. V. and Kalinina, E. P. (2001). In V. I. Makarov and V. N. Obridko (Eds.), The Sun in the Epoch of the Magnetic Field Sign Change. Sboznik Trudov Conference, St Petersburg, Russia, May 28–June 1, 2001, St Petersburg, p. 331.
Ranns, N. D. R., Harra, L. K., Matthews, S. A. and Culhane, J. L. (2001). Astron. Astrophys., 379, 616.
Ranns, N. D. R., Matthews, S. A., Harra, L. K. and Culhane, J. L. (2000). Astron. Astrophys., 364, 859.
Sterling, A. C. (1997). Astrophys. J., 478, 807.
Sterling, A. C., Harra-Murnion, L. K., Hudson, H. S. and Lemen, J. R. (1996). Astrophys. J., 464, 498.